Adiabatic and radiative cooling are both important causes of aerosol activation in simulated fog events in Europe

Pratapaditya Ghosh[1,2], Ian Boutle[3], Paul Field[3,4], Adrian Hill[3,5], Marie Mazoyer[6], Katherine J Evans[7], Salil Mahajan[7], Hyun-Gyu Kang[7], Min Xu[7], Wei Zhang[7], and Hamish Gordon[8,2]

[1]Department of Civil and Environmental Engineering, Carnegie Mellon University, 5000 Forbes Avenue, Pittsburgh, 15213, United States
[2]Center for Atmospheric Particle Studies, Carnegie Mellon University, 5000 Forbes Avenue, Pittsburgh, 15213, United States
[3]Met Office, Fitzroy Road, Exeter, EX1 3PB, United Kingdom
[4]School of Earth and Environment, University of Leeds, Leeds, LS2 9JT, United Kingdom
[5]European Center for Medium-Range Weather Forecasting, Reading, UK
[6]CNRM, Université de Toulouse, Météo-France, CNRS, Toulouse, France
[7]Oak Ridge National Laboratory, Oak Ridge, TN, 37831, USA
[8]Department of Chemical Engineering, Carnegie Mellon University, 5000 Forbes Avenue, Pittsburgh, 15213, United States
Correspondence: gordon@cmu.edu

.

Table S1: Normalized Mean Bias Factor (NMBF) for N_d for different simulations (for the 500 m model) of all fog cases.

Fog Case	Def-ARG	AD	AD-RAD	AD-RAD-SED	AD-RAD-INV	AD-RAD-DCAT
Nov 15 02:30	0.72	2.71	3.59	1.24	3.32	0.71
Nov 16 01:10	-8.96	0.22	0.35	-0.70	0.35	-1.00
Nov 16 16:00	-3.32	0.24	0.29	-0.51	0.29	-0.87
Nov 18 01:30	0.01	0.82	3.88	1.37	2.66	1.48
Nov 19 22:00	-5.20	-0.42	0.83	0.11	0.21	0.21
Nov 21 23:50	-8.76	-0.20	1.80	0.61	1.17	0.71
Nov 22 20:50	0.54	3.23	6.80	4.46	3.93	4.61
Nov 23 03:25	-0.15	0.50	0.74	-0.21	0.10	-0.42
Nov 24 06:20	0.07	0.23	1.69	-0.16	1.22	-0.19
Nov 24 16:10	-0.06	3.16	5.29	2.87	5.37	1.90
Nov 25 21:40	-3.84	-0.67	0.66	0.11	0.17	0.22

Table S2: Normalized Mean Error Factor (NMEF) for N_d for different simulations (for the 500 m model) of all fog cases.

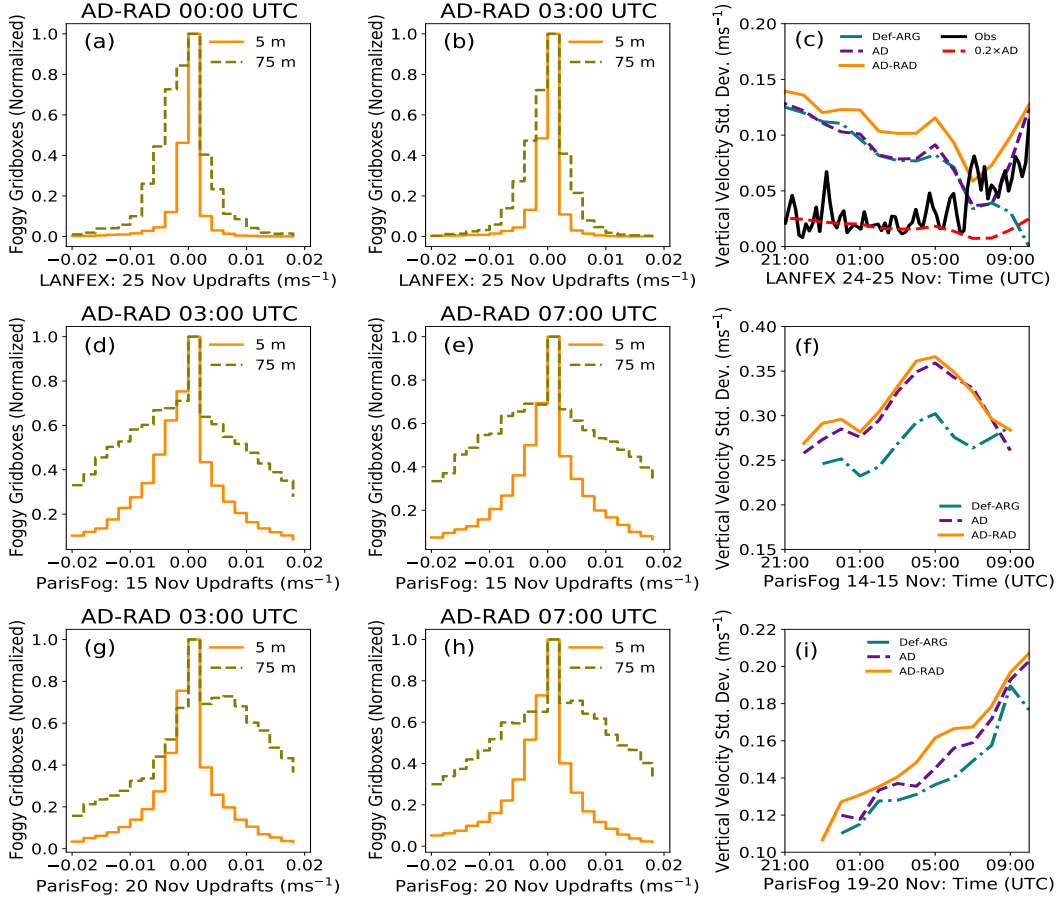| Fog Case	Def-ARG	AD	AD-RAD	AD-RAD-SED	AD-RAD-INV	AD-RAD-DCAT
Nov 15 02:30	0.99	2.76	3.64	1.29	3.37	0.97
Nov 16 01:10	9.21	0.36	0.49	1.05	0.49	1.37
Nov 16 16:00	3.46	0.30	0.33	0.72	0.33	1.11
Nov 18 01:30	0.72	1.03	3.88	1.37	2.66	1.48
Nov 19 22:00	5.86	1.01	1.37	0.86	0.86	0.95
Nov 21 23:50	9.65	0.84	1.80	0.93	1.17	1.0
Nov 22 20:50	0.85	3.23	6.80	4.46	3.93	4.61
Nov 23 03:25	0.60	0.82	0.92	0.66	0.50	0.86
Nov 24 06:20	0.72	0.81	2.12	0.60	1.64	0.60
Nov 24 16:10	2.02	3.34	5.29	2.87	5.37	1.90
Nov 25 21:40	4.20	0.97	0.84	0.63	0.62	0.67

Figure S1: Histogram of resolved updrafts (left and middle panel) at the 5 m and 75 m altitude for LANFEX and two ParisFog cases are shown here from the AD-RAD simulation. The right panel shows the simulated standard deviation (σ_w) of sub-grid updrafts (the square root of the diagnosed subgrid updraft variance) from Def-ARG, AD and AD-RAD simulations (and observations for the LANFEX case) for the same fog cases at the surface. In subfigure (c), we demonstrate that the width of the updrafts is overestimated by a factor of 5 in our simulations. This results motivates the choice of prefactor 'c' in the companion paper. These results are from the foggy gridboxes only.

Figure S2: Vertical profile of change in temperature with altitude, derived from the 500 m resolution model. The difference in temperature between two adjacent model levels in divided by the distance between the midpoints. Note the different y axis scales between different subfigures.
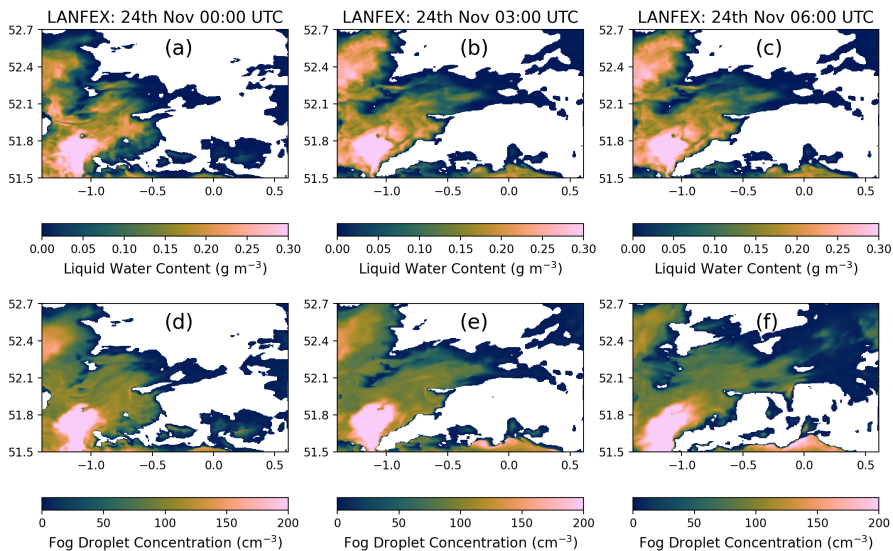

Figure S3: Spatial variation of grid-average N_d and LWC on 24 November during the LANFEX field campaign for different times (UTC). We show these properties near the surface in our 500 m model from the AD-RAD simulation.
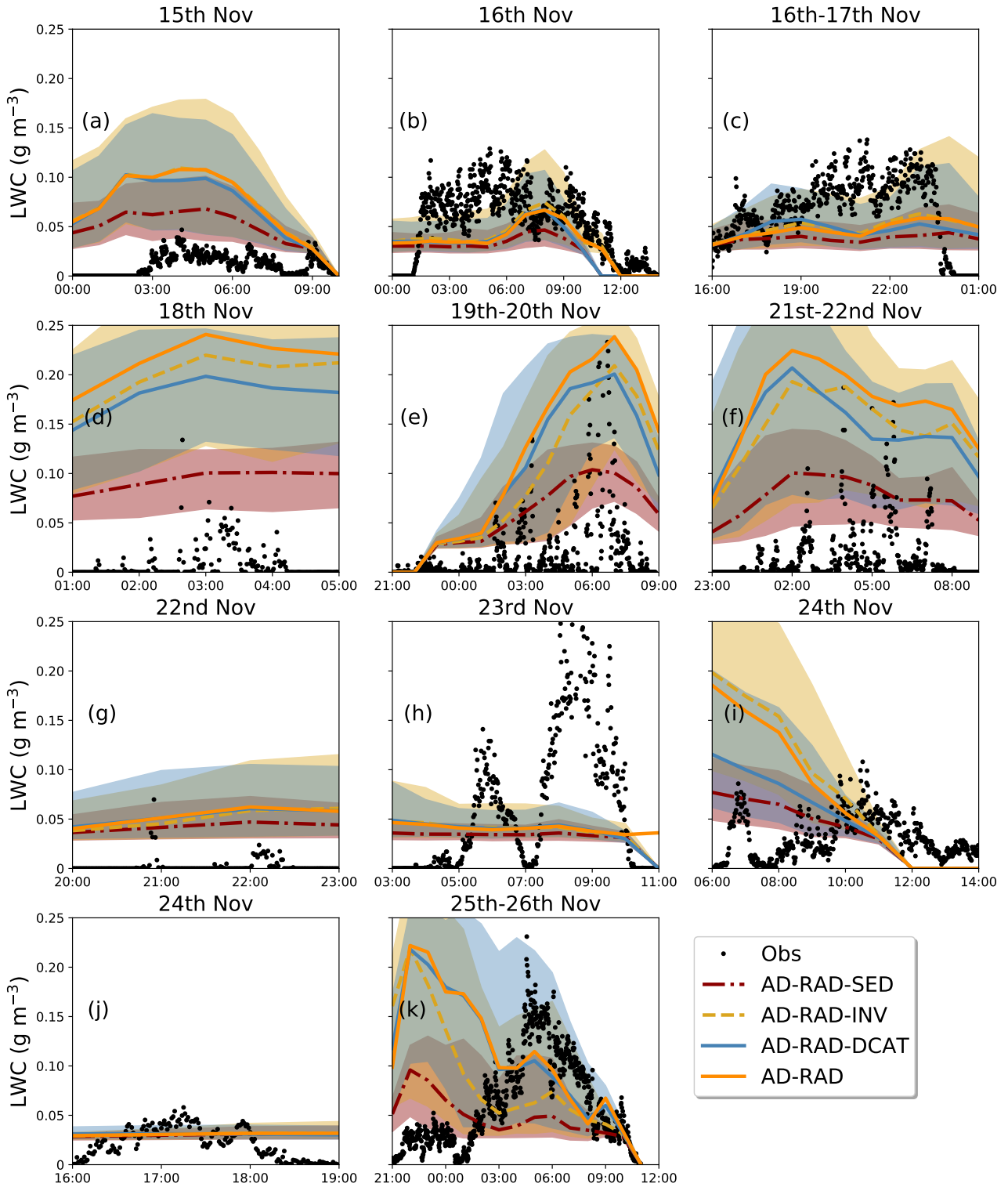
4

Figure S4: Variation of simulated and observed liquid water content as a function of time for different fog events. The results of the 500 m model near the surface from the simulations AD-RAD-SED, AD-RAD-INV, and AD-RAD-DCAT are compared with observations at the SIRTA observatory (UTC time). The solid and dashed lines represent the median values, and the shaded regions represent the interquartile ranges over the foggy gridboxes. We also show the median N_d from AD-RAD in orange solid lines for comparison.
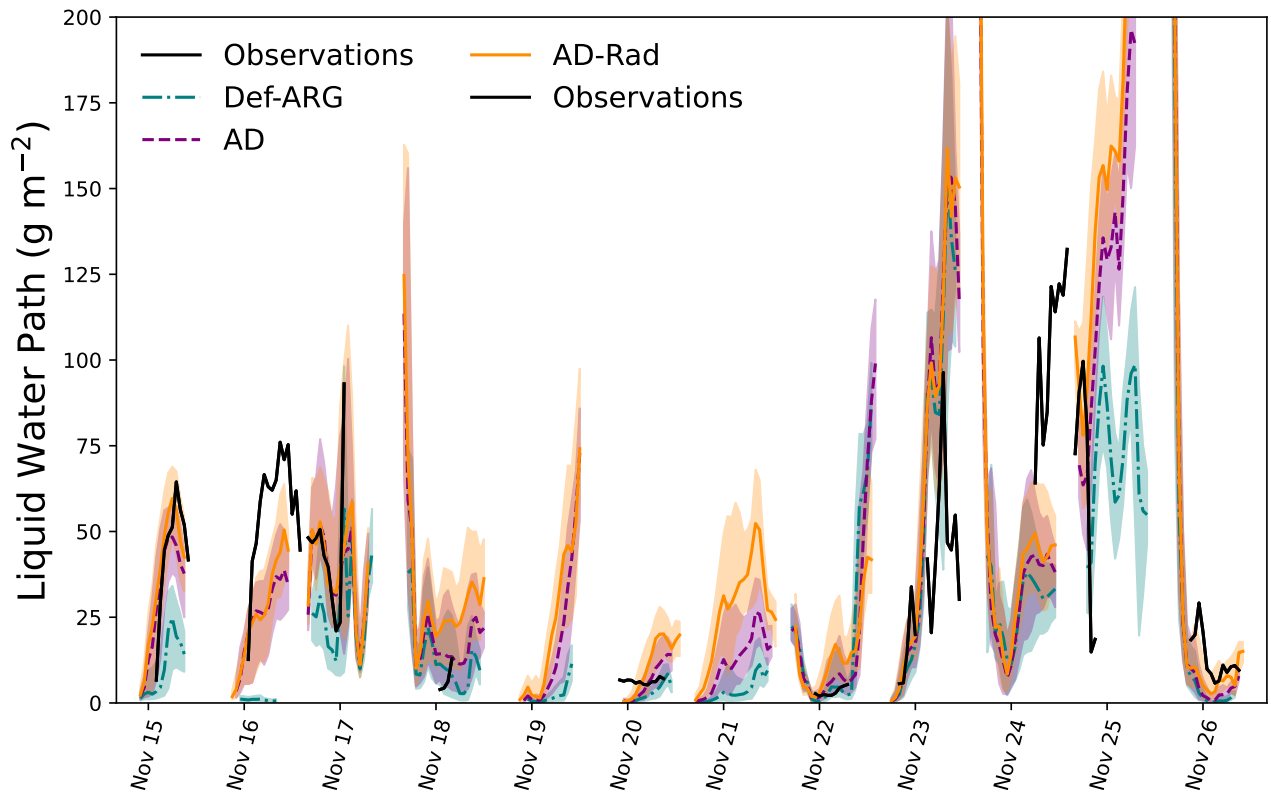
Figure S5: Time series of Liquid Water Path during the ParisFog cases with and without radiative cooling included in aerosol activation for simulations Def-ARG, AD and AD-RAD.
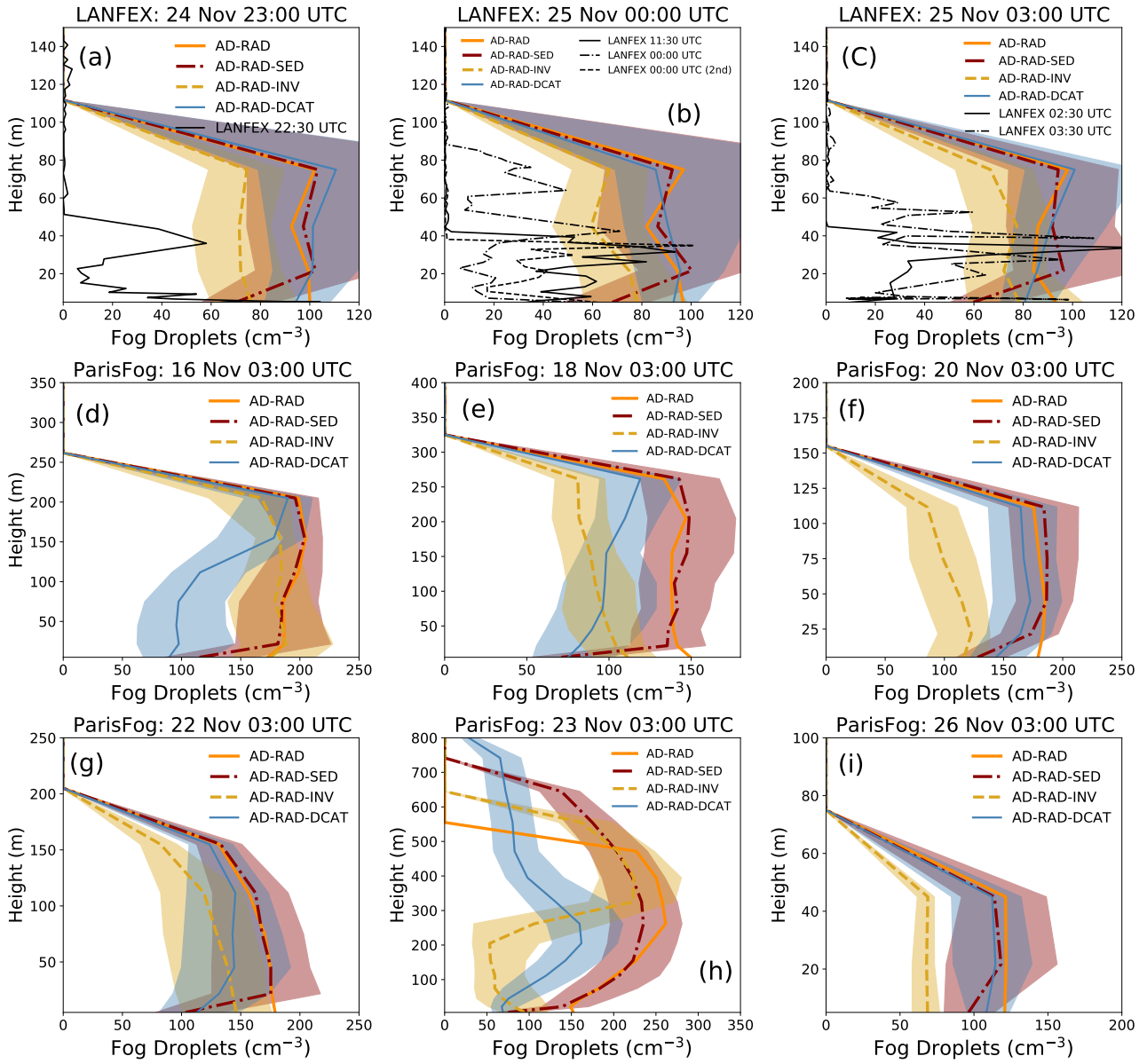
Figure S6: Vertical Profiles of N_d from the LANFEX case study and different days of the ParisFog case study. The median and interquartile range from the 500 m model for AD-RAD-SED, AD-RAD-INV, and AD-RAD-DCAT simulations are shown here. The median from AD-RAD is also plotted for comparison. Observations during LANFEX are from the fog monitor kept in the tethered balloon.
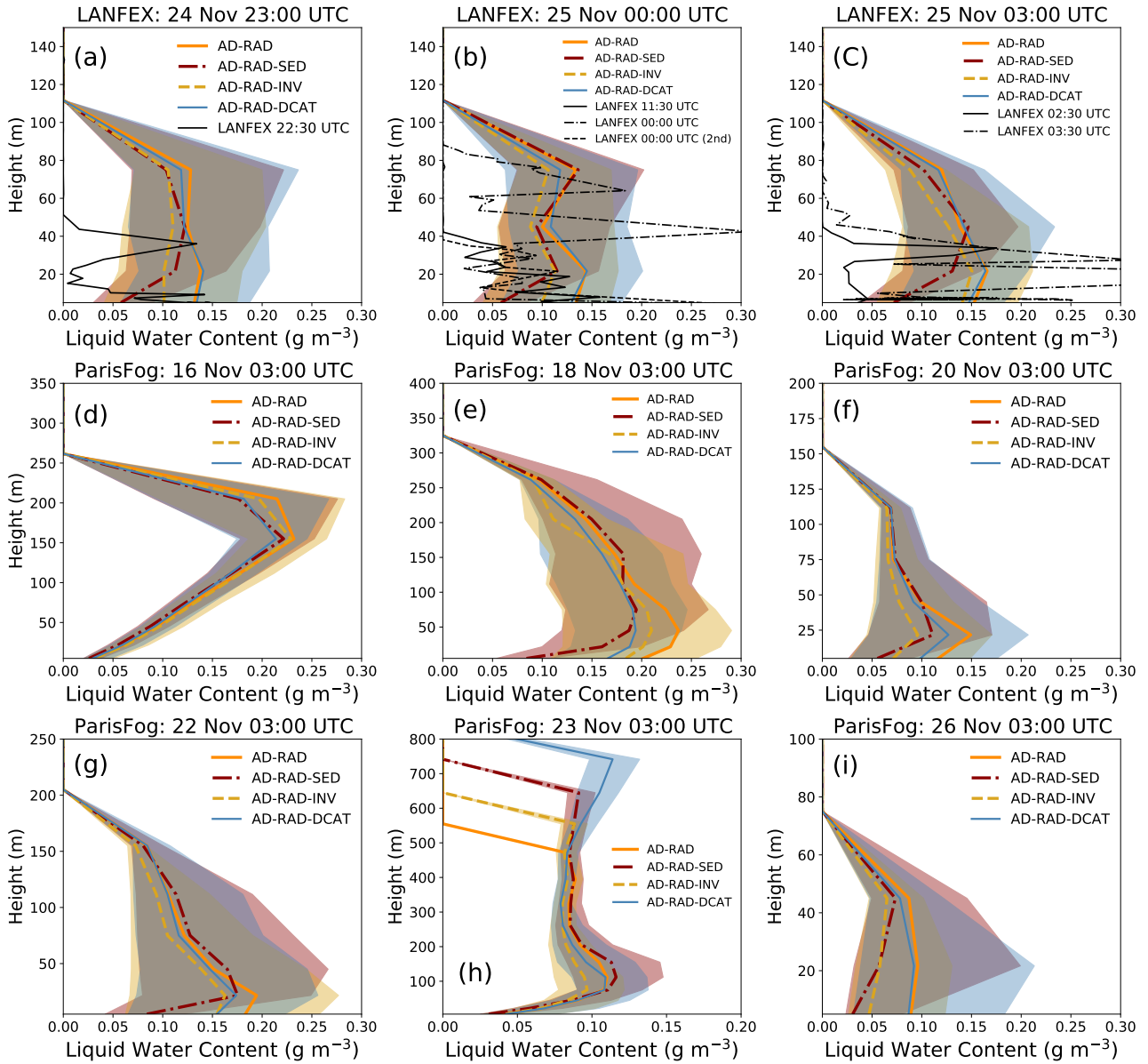
Figure S7: Vertical Profiles of LWC from the LANFEX case study and different days of the ParisFog case study. The median and interquartile range from the 500 m model for AD-RAD-SED, AD-RAD-INV, and AD-RAD-DCAT simulations are shown here. The median from AD-RAD is also plotted for comparison. Observations during LANFEX are from the fog monitor kept in the tethered balloon.
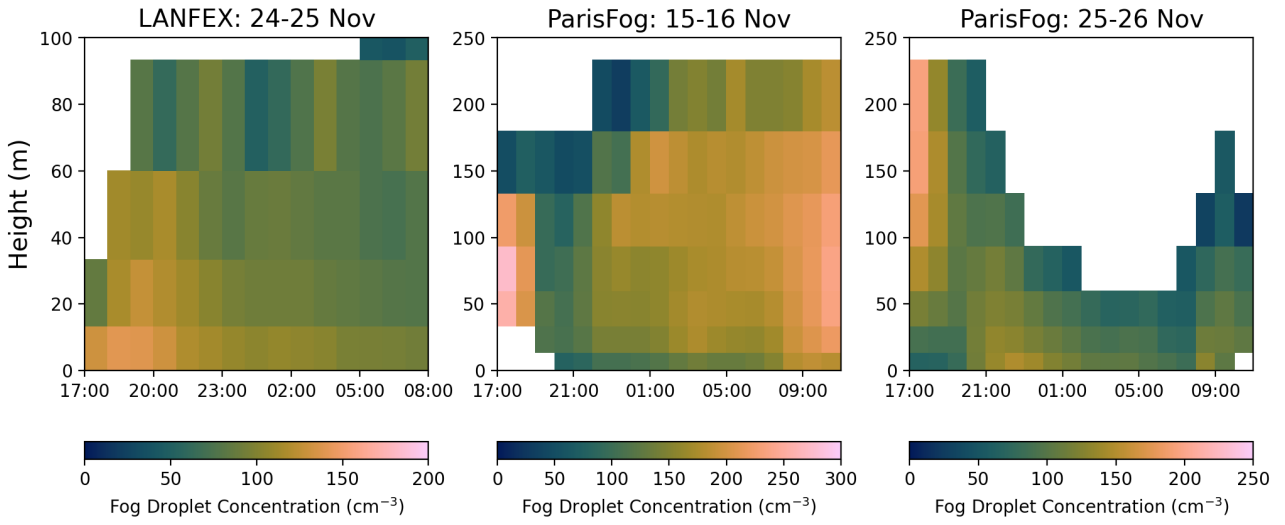
Figure S8: Vertical profile of N_d in our 500 m AD-RAD simulation, as a function of time (UTC). Left Panel: the fog event from the LANFEX case; Middle and Right Panel: Two events from the ParisFog case. The mean in-fog N_d of all foggy gridboxes (at the surface and their vertical column) are taken.
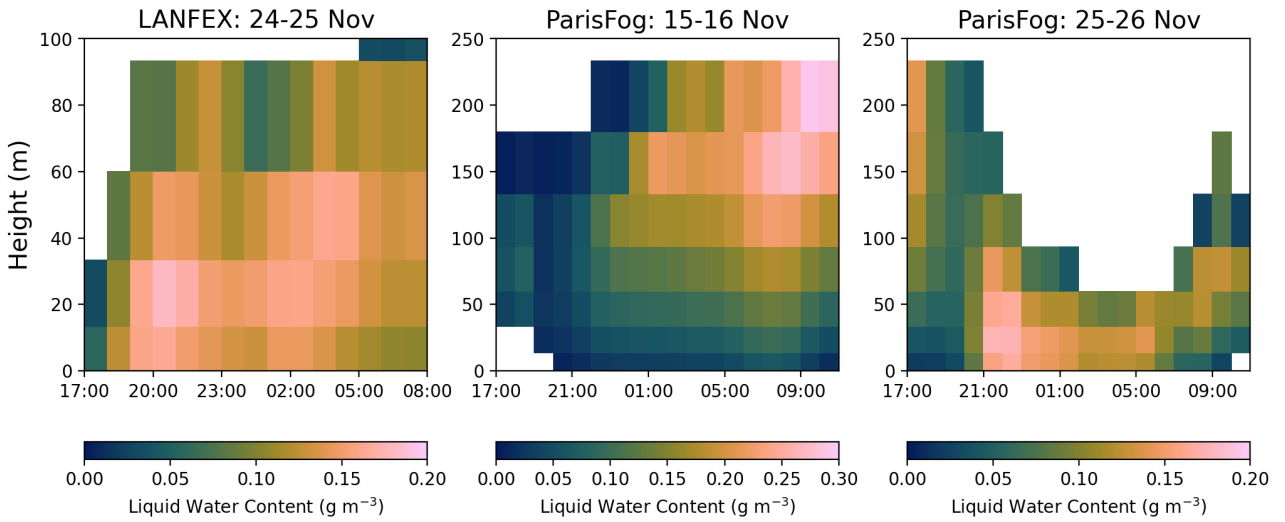

Figure S9: Vertical profile of LWC in our 500 m AD-RAD simulation, as a function of time (UTC). Left Panel: the fog event from the LANFEX case; Middle and Right Panel: Two events from the ParisFog case. The mean in-fog LWC of all foggy gridboxes (at the surface and their vertical column) are taken.

9